Progress of Theoretical Physics, Vol. 54, No. 1, July 1975

The Adler Sum Rule and Quark Parton Distribution Functions in Nucleon

Akira NIÉGAWA and Ken SASAKI†

Department of physics, Osaka City University, Osaka
†Department of Physics, Kyoto University, Kyoto

(Received December 9, 1974)

The behaviour of the quark parton distribution functions is discussed through the phenomenological analysis of the deep inelastic *e-p* and *e-n* data under constraint of the saturation of the Adler sum rule. It is concluded that in the region $0\leq x\leq x_0$ where the Regge parametrization can be applied, $\bar{u}(x)$ is equal to $\bar{d}(x)$, and both behave as const/x, (x_0 will be 0.04~0.05); for $x_0<x\leq 1$, both $\bar{u}(x)$ and $\bar{d}(x)$ reduce rapidly to sufficiently small values as x increases and $\bar{u}(x)<\bar{d}(x)$ holds; and $s(x)$ and $\bar{s}(x)$ have roughly the similar behaviour to $\bar{u}(x)$ and $\bar{d}(x)$. One possible explanation of $\bar{u}(x)<\bar{d}(x)$ for $x>x_0$ is given. The rate of convergence of the Adler sum rule is also discussed.

§ 1. Introduction and preliminaries

The first check of the *local* current-algebra in the near future, which was proposed by Gell-Mann,*) will be the Adler sum rule for neutrino processes.[2] It is derived from the local current-algebra, supplemented by some assumptions on analyticity and asymptotic behaviour of certain amplitudes:

$$\int_{q^2/2m}^{\infty} d\nu\,[W_2^{\nu p}(\nu, q^2) - W_2^{\bar{\nu} p}(\nu, q^2)] = 2(\cos^2\theta_c + 2\sin^2\theta_c), \tag{1}$$

where W_2^{lh} is one of the structure functions**) for an inelastic lepton-hadron process, $q^2(=\boldsymbol{q}^2-q_0^2)$ is the square of the momentum transferred from lepton to hadron, ν the energy transfer in the laboratory frame, m the nucleon mass and θ_c is the Cabbibo angle. Throughout this paper we set θ_c equal to zero since $\sin^2\theta_c \simeq 5\%$. Assuming the Bjorken scaling law,[4] that is, as ν and $q^2\to\infty$ with $\omega = 2m\nu/q^2$ fixed,

$$\nu W_2^{lh}(\nu, q^2) \to F_2^{lh}(\omega),$$

we can rewrite Eq. (1) as

$$\int_1^{\infty} \frac{d\omega}{\omega}[F_2^{\nu p}(\omega) - F_2^{\bar{\nu} p}(\omega)] = 2\,. \tag{2}$$

Let us call Eq. (2) the Adler sum rule (ASR) hereafter.

*) For an excellent review, see Ref. 1).
**) For their definitions in detail, for example, see Ref. 3).

In a past few years there have been several works which discuss the saturation of ASR by making use of the SLAC-MIT data on deep inelastic electron-nucleon scattering and/or by model calculations.[5] Two typical examples which were studied in the first (and also in the second) paper of Ref. 5) are the Regge pole model with the so-called counting picture of Iizuka et al.[6] and the Kuti-Weisskopf parton model,[7] both of which give remarkably slow convergence of ASR. These models satisfy the relation

$$F_2^{vp}(\omega) - F_2^{vp}(\omega) = 6(F_2^{ep}(\omega) - F_2^{en}(\omega)), \tag{3}$$

which is obtained in the former model by the assumption of the Regge pole description throughout the entire range of ω and the strong exchange degeneracy for A_2 and ρ poles, and in the latter model by the assumption of equal distributions of u- and d-type anti-quark partons (i.e., $\bar{u}(x) = \bar{d}(x)$, see below).

With the help of Eq. (3), ASR can be rewritten in terms of the structure functions of electroproduction:

$$\int_1^\infty \frac{d\omega}{\omega}(F_2^{ep}(\omega) - F_2^{en}(\omega)) = \frac{1}{3}. \tag{4}$$

The rate of convergence of the sum rule (4) is extremely slow in the above two models: In fact, 90% saturation occurs at $\omega = 413$ in the model of Iizuka et al., and at $\omega = 477$ in the Kuti-Weisskopf model.*) On the other hand, the l.h.s. of the sum rule (4) was experimentally evaluated[9] by using the data of SLAC-MIT groups up to $\omega = 20$ and by assuming the Regge form from $\omega = 20$ to ∞, and it amounted to 0.28. If ASR (2) is correct, the fact that the sum rule (4) seems difficult to be saturated leads us to consider that the relation (3) may be doubtful.

In this paper we discuss, through the phenomenological analysis of the e-p and e-n data, the saturation of ASR within the framework of the Gell-Mann-Zweig quark parton model.**),[10] Although the future neutrino and anti-neutrino experiments make it possible for us to obtain the quark parton distribution functions $u(x)$, $\bar{u}(x)$, $d(x)$, $\bar{d}(x)$ and $s(x) + \bar{s}(x)$ separately (see below for their definitions), we shall show that those behaviour can be predicted with certainty only by using the current deep inelastic electroproduction data and the constraint of

*) Some authors argue that such slow convergence of ASR seems to be unreasonable. See Ref. 8).

**) There exist other parton models which are different from one another in the way of assigning quantum numbers to partons, for example, (i) partons as fractionally charged "colored" quarks of Fritzsch and Gell-Mann;[11] (ii) partons as integrally charged Han-Nambu quarks;[12] and (iii) partons as integrally charged three-triplets of Cabibbo, Maiani and Preparata.[13] But if all hadronic states are singlets with respect to color (in the case of the model (i)) or if no "charmed" particles are produced (in the cases of the models (ii) and (iii)), the above three models cannot be distinguished from the Gell-Mann-Zweig quark parton model in the processes of deep inelastic lepton-nucleon scattering.[14]

convergence of ASR (equivalently, the convergence of the quark parton sum rules (6a) and (6b) below). In fact the sum rules (6a) and (6b) will be shown to put severe constraints upon the behaviour of $\bar{u}(x), \bar{d}(x), s(x)$ and $\bar{s}(x)$.

Now, as is well known, in the quark parton model we have[10]

$$F_2^{ep}(x) = x\left[\frac{4}{9}(u(x)+\bar{u}(x)) + \frac{1}{9}(d(x)+\bar{d}(x)) + \frac{1}{9}(s(x)+\bar{s}(x))\right], \quad (5a)$$

$$F_2^{en}(x) = x\left[\frac{1}{9}(u(x)+\bar{u}(x)) + \frac{4}{9}(d(x)+\bar{d}(x)) + \frac{1}{9}(s(x)+\bar{s}(x))\right], \quad (5b)$$

$$F_2^{\nu p}(x) = 2x[u(x)+\bar{d}(x)], \quad (5c)$$

$$F_2^{\bar{\nu} p}(x) = 2x[\bar{u}(x)+d(x)], \quad (5d)$$

where $u(x), d(x), s(x), \bar{u}(x), \bar{d}(x)$ and $\bar{s}(x)$ represent respectively the probability of finding $u, d, s, \bar{u}, \bar{d}$ and $\bar{s}$ quarks inside a *proton* with a fraction x of the nucleon longitudinal momentum in the infinite momentum frame. We have used the relation $\omega = 1/x$ which holds in parton models. The above six parton distribution functions need satisfy the following sum rules so as to conserve the total net charge, the third component of isospin and the strangeness of a proton:

$$\int_0^1 (u(x) - \bar{u}(x))\,dx = 2, \quad (6a)$$

$$\int_0^1 (d(x) - \bar{d}(x))\,dx = 1, \quad (6b)$$

$$\int_0^1 (s(x) - \bar{s}(x))\,dx = 0. \quad (6c)$$

From Eqs. (5c), (5d), (6a) and (6b), we obtain ASR (2) again. In other words, the quark parton model comprizes ASR in itself. This seems to be a natural consequence when we observe that the quark parton model is of free quark picture and that ASR is a representation of the current-algebra which is abstracted from the free quark model.

As already stated, the evaluation of the l.h.s. of Eq. (4) with the *naive* fit of the data available now does not reach to 1/3. And if $\bar{u}(x) = \bar{d}(x)$, ASR (2) can be reduced to Eq. (4) upon using Eqs. (5a)$\sim$(5d). Hence the consistency of ASR with the *naive* fit of the data of SLAC-MIT groups leads us to speculate $\bar{u}(x) \lesssim \bar{d}(x)$.

Motivated by the above preliminary considerations, we first obtain the scaling limit data on $F_2^{ep}(\omega)$ and $F_2^{en}(\omega)$ from the available SLAC-MIT electroproduction data and make a phenomenological fit in § 2. Although the behaviour of $F_2^{ep}(\omega)$ and $F_2^{en}(\omega)$, especially at large ω, is very crucial to the saturation problem of ASR, analyses already made so far do not seem to be suitable for treating the data for large ω. The available data on $\nu W_2^{ep}(q^2, \omega)$ and $\nu W_2^{en}(q^2, \omega)$ with large ω come from where the q^2's are not large, so that $\nu W_2^{ep}(q^2, \omega)$ and $\nu W_2^{en}(q^2, \omega)$

may possibly not yet scale. So we aim at careful analysis of the data in large ω region.

In § 3 we discuss the behaviour of the parton distribution functions by making use of the fit functions obtained in § 2 and the constraint of the quark parton sum rules (6a) and (6b). Through the analysis in § 3 we conclude that $\bar{u}(x)=\bar{d}(x)$ holds only for very small x, $0\leq x\leq x_0$, where the Regge parametrization can be applied, and x_0 will be 0.04~0.05; for $x_0<x\leq 1$, it must be that $\bar{u}(x)<\bar{d}(x)$ and that both take very small values and tend to zero much faster than $u(x)$ and $d(x)$ as x increases; and $s(x)$ and $\bar{s}(x)$ have roughly similar behaviour to $\bar{u}(x)$ and $\bar{d}(x)$. The behaviour of these distribution functions $\bar{u}(x), \bar{d}(x), s(x)$ and $\bar{s}(x)$ is consistent with the expectation from the experiments of $\nu(\bar{\nu})$-nucleon total cross sections at CERN[15] and FNAL.[16]

Also in § 3 we discuss the rate of convergence of ASR. Implications of our results and possible physical interpretations are discussed in § 4.

§ 2. Data analysis and determination of $F_2^{ep}(\omega)$ and $F_2^{en}(\omega)$

We need the scaling limit functions $F_2^{ep}(\omega)$ and $F_2^{en}(\omega)$, especially their accurate behaviour at large ω, because the saturation problem of ASR highly depends on the behaviour of $F_2^{ep}(\omega)$ and $F_2^{en}(\omega)$ in that region. In the following we show how we obtain the data on $F_2^{i}(\omega)$ in the scaling limit, where i stands for *ep* or *en* (in § 2.1.), and how we make a fit to get the scaling limit function $F_2^{i}(\omega)$ (in § 2.2.).*)

2.1. *Determination of scaling limit data on* $F_2^{ep}(\omega)$ *and* $F_2^{en}(\omega)$

We have used the electroproduction data**),***) of SLAC-MIT groups.[18)~21)] In translating the data given in the form of differential cross section into $\nu W_2(q^2, \omega)$,

Table I. Eight data on each *e-p* and *e-n* scattering employed from 4° scattering data of Ref. 21) are tabulated.

q^2(GeV/c)^2	ω	$\nu W_2^{ep}\pm\Delta\nu W_2^{ep}$	$\nu W_2^{en}\pm\Delta\nu W_2^{en}$
0.90	22.68	0.303 ± 0.013	0.277 ± 0.018
1.00	18.18	0.315 ± 0.011	0.282 ± 0.016
1.10	14.62	0.335 ± 0.010	0.283 ± 0.014
1.13	13.46	0.329 ± 0.009	0.280 ± 0.013
1.19	11.99	0.327 ± 0.010	0.289 ± 0.014
1.26	10.59	0.340 ± 0.004	0.284 ± 0.006
1.28	10.10	0.341 ± 0.007	0.278 ± 0.010
1.37	8.42	0.341 ± 0.006	0.284 ± 0.085

*) Contents of this section have been already discussed briefly in Ref. 17).

**) We discard some data pionts in Refs. 18) and 19) which overlap those in Ref. 20).

***) We have employed 4° scattering data, 8 points for each *e-p* and *e-n* scattering, from Ref. 21). The values of νW_2^{ep} and νW_2^{en} were found by making a one-to-one correspondence of data points in Fig. 7 to those in Fig. 8 therein. They are shown in Table I.

we adopt the experimental suggestion that $\sigma_S/\sigma_T=0.168$.*),[9] We obtain the data on $\nu W_2^{en}(q^2,\omega)$ from Ref. 20) as follows:

$$\nu W_2^{en}(q^2,\omega)=\nu W_2^{ep}(q^2,\omega)\cdot N/P\,, \tag{7}$$

where N/P is the neutron-proton cross section ratio at each data point in electron-deuteron scattering.

At present, however, the available data on $\nu W_2^{t}(q^2,\omega)$ with large ω come from where the q^2's are small, so that $\nu W_2^{t}(q^2,\omega)$ may possibly not yet scale. In what follows we show the procedures to obtain the scaling limit data which we will use in the next section 2.2 to get the scaling limit functions.

We plot all e-p (e-n) data points with $s\geq 4.84$ (GeV)^2 in the s-q^2 plane, where $s=2m\nu-q^2+m^2$. First we see the q^2-dependence of νW_2^{ep} with fixed s. We choose for s the following 14 values where sufficiently many data points are distributed: $\{s_j\}=$ (5.2, 6.3, 7.65, 9.1, 10.1, 12.3, 14.1, 15.2, 16.0, 17.75, 19.4, 21.0, 23.1 and 25.0). The data points from an experiment with a fixed incident energy and a fixed scattering angle of electron fall on a straight line in the s-q^2 plane. We obtain the value of νW_2^{ep} at the intersecting point of one of the straight lines mentioned above and a line $s=s_j$ by interpolation between the two data points which lie on the same line and are the nearest to the desired point. We apply this interpolation procedure to all the intersecting points. We also employ the extrapolation technique to obtain νW_2^{ep} at several points only when those s_j satisfy $|s_j-s_\alpha|\lesssim|s_\alpha-s_\beta|$ ($s_\beta<s_\alpha<s_j$ or $s_j<s_\alpha<s_\beta$), where s_α and s_β denote the values of s at the two nearest data points. An illustration is given in Fig. 1.

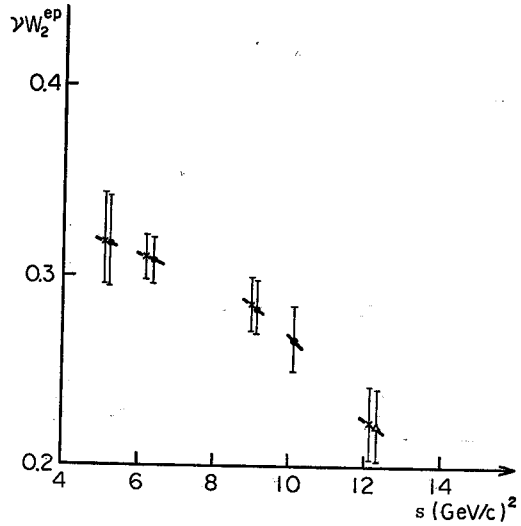

Fig. 1. A typical example of the interpolation and extrapolation procedures for νW_2^{ep} in s and q^2 ($\theta=6°$ and $E=10.0$ GeV). Crosses show experimental data, dots are the desired interpolation points and a triangle is the desired extrapolation point.

Then the q^2-dependence of νW_2^{ep} with each fixed s_j will be obtained. For each s_j we make a χ^2-fit of the form**)

*) The parton model with spin 1/2 constituents suggests that $R=r(\omega)/\nu$, (see p. 139 of Ref. 10)). But in the region where we perform the analysis, the use of $R=r(\omega)/\nu$ (with $r(\omega)=0.18m\omega$) or $R=0.168$ does not make much difference in determining $\nu W_2^{ep}(q^2,\omega)$.[9]

**) According to the analysis of Rittenberg and Rubinstein, $\omega\nu W_2^{ep}(q^2,s)$ can be fitted by a universal function of $\omega_R\equiv(s+\alpha)/(q^2+\beta)$ with free parameters α and β. See Ref. 22). At this stage we have performed fits of that kind assuming several functions, but no good fit has been obtained.

$$\nu W_2^{ep}(q^2,s_j)=a_1q^2(1+a_2q^2+a_3q^4)\exp(-a_4q^2). \tag{8}$$

The q^2-behaviour of νW_2^{ep} with $s_j=10.1$ and its fit curve are shown as a typical example in Fig. 2.

Next we observe the q^2-dependence of $\nu W_2^{ep}(q^2,\omega)$ with fixed ω. When we fix ω, there exists the point (q_j^2, s_j) corresponding to each s_j. Using the fit-function Eq. (8), we can evaluate the values of $\nu W_2^{ep}(q_j^2, s_j;\ \omega=\text{fixed})$, where $j=1, \cdots, 14$. We then perform the eyeball-fit to these $\nu W_2^{ep}(q_j^2, s_j, \omega=\text{fixed})$ as a function of q^2.*) From this fit we see that $\nu W_2^{ep}(q^2, \omega=\text{fixed})$ approaches a constant value as q^2 increases (i.e., scaling). In this way we obtain the limit value of $\nu W_2^{ep}(q^2, \omega)$ and the value $q_0^2(\omega)$ at which scaling starts for fixed ω. This procedure is applied later to seeing whether or not each datum on νW_2^{ep} (and also νW_2^{en}) is in the scaling region. A typical example is shown in Fig. 3.

We apply the same procedures to the data on νW_2^{en}. One difference is that, in this case, we choose for s_j the following 10 values: $\{s_j\}=(6.4, 7.6, 9.05, 10.7, 12.6, 14.1, 16.1, 17.75, 19.5$ and $21.3)$.

Finally we obtain the scaling limit data on $F_2^i(\omega)$ from data on $\nu W_2^i(q^2, \omega)$ in the following way: (1) We employ all data on $\nu W_2^i(q^2, \omega)$ with $q^2\geq 1$ $(\text{GeV}/c)^2$ and $s\geq 4$ $(\text{GeV})^2$; (ii) each datum on $\nu W_2^i(q^2, \omega)$ with $q^2\geq q_0^2(\omega)$ is considered to have reached the scaling limit value and is adopted as data on $F_2^i(\omega)$; (iii) when $q^2<q_0^2(\omega)$, we find from the ω-fixed-eyeball-fit the difference Δ between the limit value and the value on the curve at the same q^2 as the original data point. We then adopt the sum of Δ and the value of $\nu W_2^i(q^2, \omega)$ as data on $F_2^i(\omega)$ (see Fig. 3); (iv) we take the error of $\nu W_2^i(q^2, \omega)$ as that of data on $F_2^i(\omega)$.

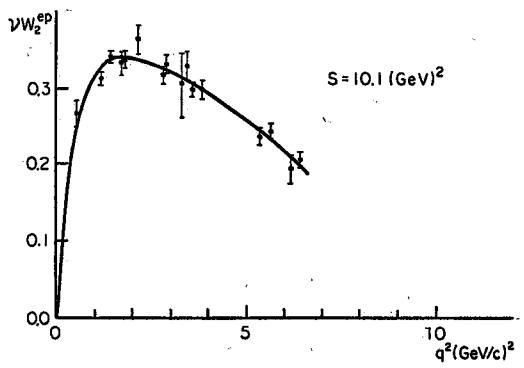

Fig. 2. The q^2-behaviour of νW_2^{ep} with s fixed $(=10.1\,(\text{GeV})^2)$ and the best fit curve.

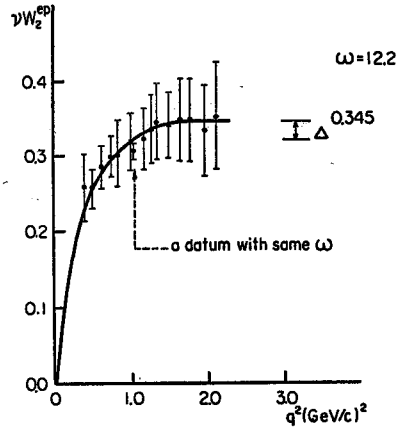

Fig. 3. The q^2-behaviour of νW_2^{ep} with ω fixed $(=12.2)$ and the eyeball-fit curve. The scaling limit and one datum with the same ω are also shown.

*) We have tried different fits of the form $\alpha q^2/(q^2+\beta)$ and $\alpha\tanh(\beta q^2)$ with α and β free parameters. But none of them have reproduced well the q^2-behaviour of νW_2^{ep} with fixed ω.

The way of modification of the data in the procedure (iii) reflects that we should take account of both the statistical fluctuation of the data and the scaling. We have modified (in the way mentioned above) 20 out of 314 data on νW_2^{ep} and 9 out of 201 data on νW_2^{en}. All modified data have $\omega > 4$.

2.2. *Scaling limit functions* $F_2^{ep}(\omega)$ *and* $F_2^{en}(\omega)$

Now we are ready to make a χ^2-fit to the scaling limit data obtained in § 2.1. and to get $F_2^{ep}(\omega)$ and $F_2^{en}(\omega)$. But it should be noted that the errors in small ω region are usually small compared with the ones at large ω. In order to obtain the fit functions as faithfully as possible at large ω, not affected by the data in small ω region, we devide the data into two groups, those with $\omega \geq \omega_0$ and the others with $\omega < \omega_0$, and we make a χ^2-fit to each group separately. We choose ω_0 as given in Table II.

Table II. The values of ω_0 we choose and fit-parameters γ_F^i and γ_A^i with their errors and the reduced χ^2 of the fits for $\omega \geq \omega_0$ are shown. The numerical results for the quark parton sum rules (6a) and (6b) by using our extreme choice of the parton distribution functions are also shown.

ω_0	1/0.06	1/0.065	1/0.07	1/0.075	1/0.08	1/0.085	1/0.09	1/0.095	1/0.1
$\gamma_F^{ep}(=\gamma_F^{en})$	0.234	0.262	0.238	0.227	0.235	0.256	0.256	0.251	0.244
	±0.057	±0.040	±0.035	±0.032	±0.028	±0.023	±0.023	±0.018	±0.017
γ_A^{ep}	0.386	0.232	0.361	0.413	0.382	0.291	0.291	0.310	0.330
	±0.263	±0.177	±0.150	±0.130	±0.112	±0.091	±0.091	±0.065	±0.059
$\gamma_A^{en}(=2\gamma_A^{ep}/3)$	0.257	0.155	0.241	0.276	0.255	0.194	0.194	0.206	0.220
	±0.175	±0.118	±0.100	±0.087	±0.075	±0.061	±0.061	±0.043	±0.039
Reduced χ^2	0.10	0.37	0.47	0.47	0.39	0.42	0.42	0.39	0.69
$\int_0^1[u(x)-\bar{u}(x)]dx$	1.73	1.51	1.63	1.66	1.61	1.47	1.44	1.44	1.45
$\int_0^1[d(x)-\bar{d}(x)]dx$	1.07	0.96	1.00	1.00	0.96	0.89	0.86	0.85	0.85

We assume the Regge behaviour of $F_2^i(\omega)$ for large $\omega(\omega \geq \omega_0)$ and that the Pomeron and the exchange-degenerate A_2-f_0 trajectories contribute to $F_2^i(\omega)$.*) Hence $F_2^i(\omega)$ is parametrized for $\omega \geq \omega_0$ as follows:

$$F_2^i(\omega) = \gamma_P^i + \gamma_A^i \omega^{-1/2}, \quad (i = ep, en) \tag{9}$$

where the zero intercepts of the Pomeron and the A_2-f_0 trajectories are assumed to be 1 and 1/2 respectively. Assuming, furthermore, the pure F coupling of the A_2-f_0 trajectory to nucleon, we can set $\gamma_A^{en} = \frac{2}{3}\gamma_A^{ep}$.

In making a χ^2-fit to the data on $F_2^i(\omega)$ *with* $\omega \geq \omega_0$ in the form of Eq. (9), we put $\gamma_P^{en} = \gamma_P^{ep}$ and $\gamma_A^{en} = \frac{2}{3}\gamma_A^{ep}$ and fit the proton and neutron data simultaneously. Next we perform a χ^2-fit to the data on $F_2^{ep}(\omega)$ and $F_2^{en}(\omega)$ with $\omega < \omega_0$ separately in the form

*) We assume that there is no Pomeron satellite term proportional to inverse power ω^{-1}.

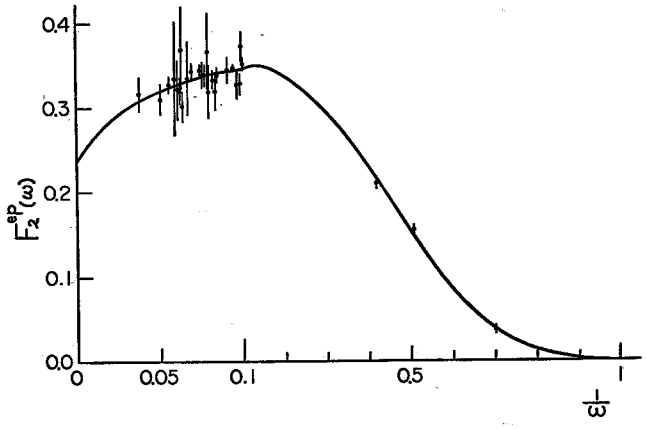

Fig. 4. All of the scaling limit data on $F_2^{ep}(\omega)$ with associated errors for $\omega \geq 10$ and a few data for $\omega < 10$ are shown. The solid line is the best fit curve when we take $\omega_0 = 1/0.07$. Note that they are plotted versus $1/\omega$ and that the region $0 < 1/\omega < 0.1$ is enlarged.

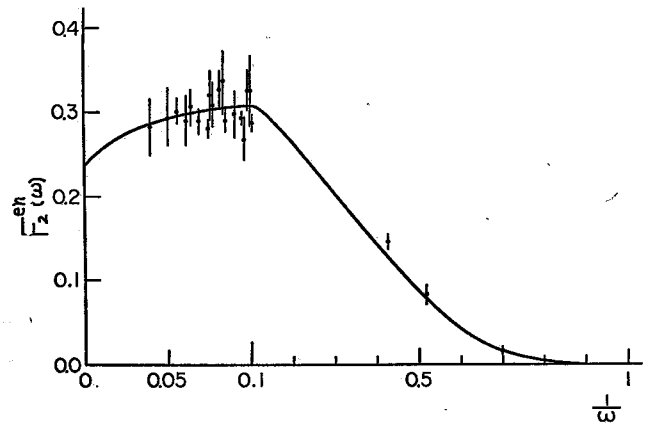

Fig. 5. All of the scaling limit data on $F_2^{en}(\omega)$ with associated errors for $\omega \geq 10$ and a few data for $\omega < 10$ are shown. The solid line is the best fit curve when we take $\omega_0 = 1/0.07$. Note that they are plotted versus $1/\omega$ and that the region $0 < 1/\omega < 0.1$ is enlarged.

$$F_2^{\,i}(\omega) = \left(1-\frac{1}{\omega}\right)^3 \sum_{k=1}^{6} b_k{}^i \left(1-\frac{1}{\omega}\right)^{k-1}, \quad (i = ep, en) \tag{10}$$

under the condition that it should join smoothly onto the fit for large ω.*) The data on $F_2^{ep}(\omega)$ and $F_2^{en}(\omega)$, the associated errors and also fit curves with ω_0 taken to be $1/0.07$ are shown in Figs. 4 and 5.

By using our fit-functions $F_2^{ep}(\omega)$ and $F_2^{en}(\omega)$, the integrals of $\int_0^1 F_2^{ep}(x)\,dx$ and $\int_0^1 F_2^{en}(x)\,dx$ can be immediately evaluated to be nearly 0.165 and 0.12 respectively. These values are in agreement with the analyses made so far.[15),23)] Also the l.h.s. of Eq. (4) is evaluated. It takes rather small value from 0.19 to 0.22 depending somewhat upon ω_0. Compare it with the value 0.28 in Ref. 9). This disagreement might be due to our modification of the data at large ω.

Finally we remark that other χ^2-fits to the data with large ω have also been performed: (i) A fit with $\gamma_A{}^{ep}$ and $\gamma_A{}^{en}$ treated as free parameters; (ii) a fit with

*) The reduced χ^2 of the fits for $\omega < \omega_0$ ranges from 2.0 to 2.3 for $i=ep$ and from 1.5 to 1.8 for $i=en$.

three terms, added one more term $\gamma_A{}^i\omega^{-3/2}$, which is the sum of the contribution of the A_2'-trajectory with zero intercept $-1/2$, the possible satellite term of the A_2-f_0 pole and everything else, and with the constraints of $\gamma_P{}^{en}=\gamma_P{}^{ep}$ and $\gamma_A{}^{en}=\frac{2}{3}\gamma_A{}^{ep}$; (iii) A fit with three terms and with only one constraint of $\gamma_P{}^{en}=\gamma_P{}^{ep}$. Since the errors in large ω region are not small, fit parameters highly depend on ω_0 and we cannot say any definite conclusion at the present stage of the data accumulation.

§ 3. Distribution functions of quark partons

In this section, with scaling limit functions $F_2{}^{ep}(\omega)$ and $F_2{}^{en}(\omega)$ obtained in § 2.2. and with the quark parton sum rules (6a) and (6b), we discuss the behaviour of parton distribution functions and also the rate of convergence of ASR.

In the framework of the quark parton model, ASR (2) can be derived from quark parton sum rules (6a) and (6b). Let us, therefore, examine these two sum rules. As implied in the discussion in § 1, the experimentally evaluated value of the integral of Eq. (4) is less than 1/3 (much less than 1/3 in our analysis), and there is a doubt that the current electroproduction data may not be compatible with the saturation of the quark parton sum rules. Therefore we try to divide scaling limit functions $F_2{}^{ep}(\omega)$ and $F_2{}^{en}(\omega)$ into parton distribution functions *so that they may serve most favourably the saturation of sum rules (6a) and (6b).* (Resultant parton distributions are therefore unrealistic.) First we set $s(x)=\bar{s}(x)=0$. Then, using Eqs. (5a) and (5b), we can solve for $u(x)+\bar{u}(x)$ and $d(x)+\bar{d}(x)$. Further, these distribution functions are divided into $u(x)$, $\bar{u}(x)$, $d(x)$ and $\bar{d}(x)$ so that the integrals of Eqs. (6a) and (6b) may reach maximum.

Here we should note that when we made a fit to obtain the scaling limit functions $F_2{}^{ep}(\omega)$ and $F_2{}^{en}(\omega)$ in § 2.2, we performed Regge parametrization for $0\leq x\leq x_0(x_0\equiv 1/\omega_0)$. We assumed that there is no first satellite term of Pomeron and no Pomeron-P' cut (i.e., no term proportional to inverse power ω^{-1}). Then $\bar{u}(x)$ and $\bar{d}(x)$ should be equal and proportional to $1/x$ for $0\leq x\leq x_0$. The proportional constant is given by $9\gamma_P{}^{ep}/10$ (note $\gamma_P{}^{ep}=\gamma_P{}^{en}$) which is derived from Eqs. (5a) and (5b) and from a constraint that $x\bar{u}(x)$ and $xu(x)$ should be equal at $x=0$. In order to maximize the l.h.s. of Eqs. (6a) and (6b), we set, though unrealistic, $\bar{u}(x)=\bar{d}(x)=0$ for $x_0<x\leq 1$. The values of the integrals (6a) and (6b) in this extreme case are shown in Table II.

Even though we took the extreme choice of parton distribution functions, we shall see from Table II that the l.h.s. of Eq. (6a) is still short of saturation by 15% or more. One thing to be noteworthy is that the saturation of Eq. (6b) is better than that of Eq. (6a) in every choice of x_0. In fact, in the cases $x_0=0.06$, 0.07 and 0.075, our extreme choice of parton distribution functions makes it possible to saturate the l.h.s. of Eq. (6b) completely.

In the cases of other fits mentioned at the end of § 2.2, the fit parameters,

and hence the saturation of the sum rules (6a) and (6b) highly depend upon x_0. But the situation that the saturation of Eq. (6b) is better than that of Eq. (6a) does not change in all of the fits.

From the analysis we have made so far, we see that as long as our method of fit parametrization is suitable, x_0 must be taken still smaller, say 0.05 or less, in order to saturate the quark parton sum rules and also to obtain reasonable parton distribution functions. This means that ω_0 (at $\omega > \omega_0$, Regge parametrization is justified) goes farther away. Therefore we need further accumulation of the deep inelastic scattering data with still larger ω. But from the arguments made in this section we can predict with certainty the behaviour of the parton distribution functions as follows: For $0 \leq x \leq x_0$, $\bar{u}(x) = \bar{d}(x)$ and they behave as const/x. For $x_0 < x \leq 1$, $\bar{u}(x)$ and $\bar{d}(x)$ must be very small and tend rapidly to zero compared with $u(x)$ and $d(x)$ as x increases. Otherwise the saturation of quark parton sum rules would become difficult. Another thing we should note is that, for $x_0 < x \leq 1$, $\bar{d}(x) > \bar{u}(x)$ and accordingly the relation (3) and Eq. (4) will not hold.[24] This is supported by the fact that in our extreme choice of the parton distribution functions the saturation of the sum rule (6b) has been much better than the other one (6a). The distribution functions of $s(x)$ and $\bar{s}(x)$ must show similar behaviour to those of $\bar{u}(x)$ and $\bar{d}(x)$ for $x_0 < x \leq 1$. For $0 \leq x \leq x_0$, the argument of $SU(3)$ symmetry suggests that $s(x)$ and $\bar{s}(x)$ have the same behaviour as $\bar{u}(x)$ and $\bar{d}(x)$. Or if we can apply here the argument of Carlitz, Green and Zee,[25] it is concluded that $s(x) = \bar{s}(x) \cong 0.6\bar{u}(x)$ $(= 0.6\bar{d}(x))$. The behaviour of these parton distribution functions $\bar{u}(x)$, $\bar{d}(x)$, $s(x)$ and $\bar{s}(x)$ is compatible with the expectation from the experiments of $\nu(\bar{\nu})$-nucleon total cross sections at CERN[15] and FNAL.[16]

When $\bar{d}(x) > \bar{u}(x)$, Eq. (4) is replaced by an inequality:

$$\int_1^\infty \frac{d\omega}{\omega}[F_2^{ep}(\omega) - F_2^{en}(\omega)] < \frac{1}{3}. \tag{11}$$

This will improve the convergence of ASR as compared with the case in which Eq. (4) holds. But our analysis in this section suggests that the rate of convergence will be still slow, with the value of ω not less than 100 for 90% saturation. The reason for this is the following. We calculate Ω, which is defined by

$$\frac{1}{2}\int_0^{\Omega^{-1}}[u(x) - \bar{u}(x)]dx = \int_0^{\Omega^{-1}}[d(x) - \bar{d}(x)]dx = 0.1,$$

with our (extreme) choice of parton distribution functions to get $\Omega = 22 \sim 68$. If we restrict ourselves to the cases in which the values of l.h.s. of Eq. (6a) are larger than 1.6, we get $\Omega = 52 \sim 68$. Taking into account the fact that in the real world the contribution from the region $x \geq x_0$ to the integrals (6a) and (6b) is smaller than that of our extreme case, the 90% saturation of the quark parton

sum rules, or ASR, will be achieved at Ω not less than 100. This makes a clear contrast to the arguments for early saturation of ASR.[8]

In concluding this section we add a remark that when the data with larger ω are accumulated, there is a possibility that the 3-term fit, added a low-lying A_2' trajectory contribution, may give the better fit than the 2-term fit. If that is the case, a possibility remains that the early saturation of ASR may be realized.*)

§ 4. Summary and discussion

In this paper we are concerned with the behaviour of the parton distribution functions under the constraint of ASR, more specifically, quark parton sum rules (6a) and (6b). By keeping in mind that the accurate behaviour of the scaling limit functions $F_2^{ep}(\omega)$ and $F_2^{en}(\omega)$ in large ω region is necessary to the saturation problem of ASR, the scaling limit data on $F_2^{ep}(\omega)$ and $F_2^{en}(\omega)$ were obtained from the available electroproduction data of SLAC-MIT groups and the phenomenological fits were made (in § 2). Then the extreme case of parton distribution functions was taken (though unrealistic) so that the l.h.s. of the parton sum rules (6a) and (6b) should be maximized: That is, $s(x)=\bar{s}(x)=0$ for all x, $\bar{d}(x)=\bar{u}(x)=\text{const}/x$ for $0\leq x\leq x_0$ and $\bar{d}(x)=\bar{u}(x)=0$ for $x_0<x\leq 1$, and the evaluation of the integrals was made. Even with such an extreme case, the l.h.s. of Eq. (6a) was found to come short of saturation by about 15% or more. On the other hand, the l.h.s. of Eq. (6b) was saturated or almost saturated (it depends somewhat upon x_0).

Through this analysis, we found that ω_0 (at $\omega>\omega_0$, Regge parametrization can be applied) should run farther away, say $\omega_0=25\sim 30$. So further accumulation of data with larger ω will be needed. But based upon the present analysis the following behaviour of the parton distribution functions can be reasonably predicted: (i) For $0\leq x\leq x_0$, $\bar{d}(x)=\bar{u}(x)$, and both behave as const/x, and for $x_0<x\leq 1$, both $\bar{d}(x)$ and $\bar{u}(x)$ are much smaller and tend more rapidly to zero than $u(x)$ and $d(x)$ as x increases; (ii) For $x_0<x\leq 1$, it holds that $\bar{u}(x)<\bar{d}(x)$. Hence the relation (3) and the sum rule (4) will fail. (iii) $s(x)$ and $\bar{s}(x)$ have roughly a similar behaviour to $\bar{u}(x)$ and $\bar{d}(x)$.

It is interesting here to see what the above statement (ii) will suggest. A few years ago, one of the present authors (A.N.)[27] proposed an idea, concerning one of the possibilities to explain the behaviour of $F_2^{en}(\omega)/F_2^{ep}(\omega)$ near the threshold region $\omega\approx 1$, that quark parton obey a certain statistics with the exclusion principle. We briefly present the argument here.

In many quark parton models,[7),28] the diagrams in which the current couples to one of the valence quarks dominate in the region $x\approx 1$. If we assume that the exclusion principle works among the partons of the same kind with almost the same momentum fraction, the configuration in which the leading parton (its

*) In fact, such models are reported, see for example Ref. 26).

momentum fraction $x\approx 1$) is d-quark will be suppressed in comparison with the configuration where the leading parton is u-quark. The reason is that in the former case residual valence partons (both have $x\approx 0$) are of the same kind, uu and in the latter they are of a different kind, ud. Here we have assumed that there is no long range correlation between the leading parton and the residual partons. Then the suppression of $d(x)$ relative to $u(x)$ near the region $x\approx 1$ leads through Eqs. (5a) and (5b) to that as $x\to 1$, $F_2^{en}(\omega)/F_2^{ep}(\omega)$ reduces to the value less than 2/3 which is the ratio given by the "naive" counting of the three valence quarks.

The argument along the same line also serves to be one of the possibilities to explain that $\bar{u}(x)<\bar{d}(x)$ for "moderate" x. Let us consider two cases of the lowest configuration which is made up of three "valence" partons plus one pair of "sea" partons: The one is $u_1u_2d_3+(u_4\bar{u}_5)$ (case A) and the other is $u_1u_2d_3+(d_4\bar{d}_5)$ (case B). We have labeled the partons of each configuration as 1, 2, 3, 4 and 5. Each parton carries a fraction of x_i $(i=1, 2, \cdots, 5)$ of the longitudinal momentum of a proton. By neglecting the transverse momentum, spins and other internal degrees of freedom of partons,*) the amplitudes of these configurations are expressed as functions of only momentum fraction x_i of partons: $F_{(A)}(\{x_i\})$ for case A and $F_{(B)}(\{x_i\})$ for case B.

Again we assume the exclusion principle among quark partons of the same kind and the absence of the (long range) correlation between the leading parton and the residual partons. Then in case A when $\bar{u}_5$ is a leading parton (say, $x_5>1/5$) and the residual partons have the small x's, the amplitude may possibly be written as

$$F_{(A)}(\{x_i\})\sim(1-x_5)^{\beta/2}(x_1x_2x_3x_4)^{\alpha/2}(x_1-x_2)(x_2-x_4)(x_4-x_1), \quad (12a)$$

and in case B when $\bar{d}_5$ is a leading parton, we may obtain

$$F_{(B)}(\{x_i\})\sim(1-x_5)^{\beta/2}(x_1x_2x_3x_4)^{\alpha/2}(x_1-x_2)(x_3-x_4), \quad (12b)$$

where α and β are some real numbers. The contribution of the configurations (case A) and (case B) to the parton distribution functions $\bar{u}(x)$ and $\bar{d}(x)$ can be calculated respectively to be

$$\bar{u}_{(A)}(x)=\int_0^1\prod_{i=1}^5\frac{dx_i}{x_i}\delta(1-\sum_{i=1}^5 x_i)|F_{(A)}(\{x_i\})|^2\delta(x_5-x), \quad (13a)$$

$$\bar{d}_{(B)}(x)=\int_0^1\prod_{i=1}^5\frac{dx_i}{x_i}\delta(1-\sum_{i=1}^5 x_i)|F_{(B)}(\{x_i\})|^2\delta(x_5-x). \quad (13b)$$

Inserting (12a) and (12b) into Eqs. (13a) and (13b), respectively, we find that $\bar{u}_{(A)}(x)<\bar{d}_{(B)}(x)$ for "moderate" x, say $x>1/5$. This argument can also be ap-

*) Even when we take into account transverse momenta, spins and other internal degrees of freedom of partons the discussion here is still applicable to the amplitudes which are symmetric with respect to those degrees of freedom.

plied to the cases where we consider the contributions of the higher configurations with many "sea" partons toward $\bar{u}(x)$ and $\bar{d}(x)$. Summing up all the contributions, we reach $u(x)<d(x)$ for "moderate" x.

Although our arguments are based on the validity of quark parton sum rules (6a) and (6b), and hence on that of ASR(2), there have been several works where ASR itself is criticized and/or its alternatives are presented.[29] Also one possibility was discussed that the original ASR(1) is correct but the sum rule (2) which we call ASR in this paper does not hold.[30] If any one of the above possibilities comes true in our physical world, then the parton ideas would topple down.

Acknowledgements

The authors would like to thank Dr. H. Nakajima for a careful reading of the manuscript. One of the authors (A. N.) thanks the Sakkokai Foundation for financial support.

References

1) S. L. Adler and R. F. Dashen, *Current Algebras and Applications to Particle Physics* (Benjamin, New York, 1968).
2) S. L. Adler, Phys. Rev. **143** (1966), B1144.
3) D. Gross and C. H. Llewellyn-Smith, Nucl. Phys. **B14** (1969), 337.
4) J. D. Bjorken, Phys. Rev. **179** (1969), 1547.
5) J. D. Bjorken and S. F. Tuan, Comments on Nuclear and Particle Physics **5** (1972), 70.
J. J. Sakurai, H. B. Thacker and S. F. Tuan, Nucl. Phys. **B48** (1972), 353.
S. F. Tuan, Phys. Rev. **D7** (1973), 2092.
R. McElhaney and S. F. Tuan, Phys. Rev. **D8** (1973), 2267.
E. A. Paschos, *Proceedings of the 16th International Conference on High Energy Physics, Chicago-Batavia, Ill. 1972*, ed. J. D. Jackson and A. Roberts (NAL, Batavia, Ill.), vol. 2, p. 166.
O. Nachtmann, Phys. Rev. **D7** (1973), 3340.
6) J. Iizuka, M. Kobayashi and H. Nitto, Prog. Theor. Phys. **45** (1971), 482.
7) J. Kuti and V. F. Weisskopf, Phys. Rev. **D4** (1971), 3418.
8) P. Langacker and M. Suzuki, Phys. Letters **40B** (1972), 561.
M. Suzuki, Nucl. Phys. **B66** (1973), 368.
H. T. Nieh, Phys. Rev. **D1** (1970), 3161.
9) E. D. Bloom, *Proceedings of the 6th International Symposium on Electron and Photon Interactions at High Energies, Bonn, 1973*, ed. H. Rollnik and W. Pfeil, p. 227.
10) R. P. Feynman, Photon-Hadron Interactions (W. A. Benjamin Inc., 1972).
11) M. Gell-Mann, XI Intern. Universitätswochen für Kernphysik, Schladming (1972).
12) M. Y. Han and Y. Nambu, Phys. Rev. **139** (1965), B1006.
13) N. Cabibbo, L. Maiani and G. Preparata, Phys. Letters **B25** (1967), 132.
14) H. J. Lipkin, Phys. Rev. Letters **28** (1972), 63.
M. Koca and M. S. K. Razmi, Phys. Rev. **D8** (1973), 4142.
M. Y. Han and Y. Nambu, Phys. Rev. **D10** (1974), 674.
15) D. H. Perkins, *Proceedings of the 16th International Conference on High Energy Physics, Chicago-Batavia, Ill. 1972*, ed. J. D. Jackson and A. Roberts (NAL, Batavia, Ill.), vol. 4, p. 189.

16) A. Benvenuti et al., Phys. Rev. Letters **32** (1974), 125.
17) A Niégawa and K. Sasaki, Lett. Nuovo Cim. **11** (1974), 221.
18) M. Breidenbach, MIT thesis, MIT Report No. MIT-2098-635 (1970).
19) G. Miller, Stanford thesis, SLAC Report No. SLAC-129 (1971).
20) A. Bodek, MIT thesis, MIT Report No. COO-3069-116 (1972).
21) E. D. Bloom, CALT preprint CALT-68-392 (1973).
22) V. Rittenberg and H. Rubinstein, Phys. Letters **B35** (1971), 50.
F. W. Brasse et al., Nucl. Phys. **B39** (1972), 421.
23) V. Barger and R. J. N. Phillips, Nucl. Phys. **B73** (1974), 269.
24) J. Pestieau and J. J. Salasar, Lett. Nuovo Cim. **6** (1973). 351.
25) R. Carlitz, M. B. Green and A. Zee, Phys. Rev. **D4** (1971), 3439.
26) M. Suzuki, Nucl. Phys. **B66** (1973), 368.
See also R. McElhaney and S. F. Tuan, Phys. Rev. **D8** (1973), 2267.
27) A. Niégawa, Lett. Nuovo Cim. **6** (1973), 81.
28) J. D. Bjorken and E. A. Paschos, Phys. Rev. **185** (1969), 1975.
G. Altarelli et al., Nucl. Phys. **B69** (1974), 531.
J. F. Gunion, Phys. Rev. **D10** (1974), 242.
29) G. W. Barry, G. J. Gounaris and J. J. Sakurai, Phys. Rev. Letters **21** (1968), 941.
See also:
S. Mukherjee, Lett. Nuovo Cim. **7** (1973), 139.
A-M. M. Abdel-Rahman, Nuovo Cim. **19A** (1974), 53.
H. Harari, Phys. Rev. Letters **22** (1969), 1078.
A. Khare and K. Kawarabayashi, Prog. Theor. Phys. **52** (1974), 263.
30) J. Genova, Phys. Rev. **D9** (1974), 1065.
See also, J. M. Cornwall, D. Corrigan and R. E. Norton, Phys. Rev. **D3** (1971), 536.
31) R. P. Feynman, *Proceedings of the Fifth Hawaii Topical Conference in Particle Physics, Hawaii, 1973*, p. 1; Summary talk given at International Conference on Neutrino Physics and Astrophysics, Philadelphia, PA, 1974.
32) F. J. Sciulli, CALT preprint CALT-68-450.

Note added:

After completion of this work we become aware of the reports of Feynman and Sciulli.[31),32)] Feynman gave in his reports a rough sketch of the x-dependences of the functions $q(x)\equiv x(u(x)+d(x))$ and $\bar{q}(x)\equiv x(\bar{u}(x)+\bar{d}(x))$: $\bar{q}(x)$ is a monotone decreasing function of x and $\bar{q}(x\approx 0.05)\approx\bar{q}(x=0)/e$. Analysing the CERN-Gargamelle neutrino data, Sciulli concluded that $\bar{q}(x)\ll q(x)$ for $x\gtrsim 0.05$. If these are the case, x_0, which is the upper limit value of the Regge region $x\leq x_0$, if any, should be extremely small.

The numerical calculations were performed by FACOM 230-75 at the Computer Center, Kyoto University and by FACOM 270-30 at the Computer Center, Osaka City University.